

This implies that the solution completely fills the tubes. Our method opens the way to filling the internal volume of nanotubes with a wide variety of materials using solutions of their precursors. □

Received 5 September; accepted 12 October 1994.

1. Iijima, S. *Nature* **354**, 56–58 (1991).
2. Ebbesen, T. W. & Ajayan, P. M. *Nature* **358**, 220–222 (1992).
3. Dresselhaus, M. S. *Nature* **358**, 195–196 (1992).
4. Ruoff, R. S., Lorents, D. C., Chan, B., Malhotra, R. & Subramoney, S. *Science* **259**, 346–348 (1993).

5. Tomita, M., Saito, Y. & Hayashi, T. *Jap. J. appl. Phys.* **32**, L280–L282 (1993).
6. Seraphin, S., Zhou, D., Jiao, J., Withers, J. C. & Loufty, R. *Nature* **362**, 503 (1993).
7. Saito, Y. *et al. Chem. Phys. Lett.* **209**, 72–76 (1993).
8. Saito, Y. *et al. J. Phys. Chem. Solids* **54**, 1849–1860 (1993).
9. Murakami, Y. *et al. J. Phys. Chem. Solids* **54**, 1861–1870 (1993).
10. Ajayan, P. M. & Iijima, S. *Nature* **361**, 333–334 (1993).
11. Tsang, S. C., Harris, P. J. F. & Green, M. L. H. *Nature* **362**, 520–522 (1993).
12. Ajayan, P. M. *et al. Nature* **362**, 522–525 (1993).
13. Harris, P. J. F., Green, M. L. H. & Tsang, S. C. *J. chem. Soc., Faraday Trans.* **89**, 1189–1192 (1993).

ACKNOWLEDGEMENTS. We thank P. G. Dickens, P. D. Battle, J. B. Claridge and R. M. Lago for discussions; we are grateful for the use of a JEOL 4000EX high-resolution transmission electron microscope in the Department of Materials, University of Oxford.

Role of the thermohaline circulation in the abrupt warming after Heinrich events

D. Paillard* & L. Labeyrie†

* Laboratoire de Modélisation du Climat et de l'Environnement, CEA/DSM CE Saclay, 91191 Gif sur Yvette Cedex, France
† CFR Laboratoire mixte CNRS-CEA, Domaine du CNRS, 91198 Gif sur Yvette Cedex, France

EVIDENCE of rapid climate oscillations during the last glacial period has been identified in climate records from Greenland ice cores^{1,2} and ocean sediments in the North Atlantic^{3,4}. These records show that periods of gradual cooling are terminated by abrupt warming events⁵, with the coldest periods coinciding with the deposition of ice-rafted debris (so-called Heinrich events) throughout the North Atlantic. Heinrich events are thought to be a signature of massive iceberg discharges owing to collapse of the Laurentide ice sheet; Bond *et al.*⁵ have proposed that the decrease in meltwater flux following collapse and retreat of the ice sheet enhanced the ocean's thermohaline circulation⁶, thereby increasing advection of heat from the tropics and giving rise to abrupt climate warming. Here we test this idea using a simple ocean model coupled to a model of a periodically surging ice sheet. We find that massive discharges of icebergs first stop the thermohaline circulation because of the consequent freshwater influx, cooling the North Atlantic region. This is followed by a rapid restart of the circulation, leading to abrupt warming. Thus our model can reproduce the qualitative features of the climate oscillations seen in the ice-core and ocean records.

The so-called 'Dansgaard-Oeschger events' were first seen as abrupt shifts in the oxygen isotope ratio of three Greenland ice cores, from Camp Century, Dye 3 and Renland. Two new cores, GRIP^{1,7} and GISP2⁸, recently confirmed these rapid excursions in $\delta^{18}\text{O}$, which reflect changes in the temperature of formation of local precipitation^{1,9}. Furthermore, marine sediments in many cores over the North Atlantic exhibit layers of detritic materials³. These materials came largely from the margins of the Labrador Basin¹⁰; transport to lower latitudes is explained by enhanced discharge of icebergs and subsequent melting. During these deposition events, the sea surface temperature was considerably cooler^{4,5}. Therefore, both ice-core and marine-sediment data strongly suggest rapid climate oscillations during glacial periods. The periodicities of the 'Dansgaard-Oeschger events' vary from 1 to 10 kyr, and the longer-term cycles (7–10 kyr) culminate at the same time as Heinrich events. Figure 3 of ref. 5 shows that iceberg discharge indeed occurs when temperatures over Greenland, as well as sea surface temperatures, are around their minima. These features are observed throughout the glacial period and even during the deglaciation. Some continental records¹¹ correlate well with these longer-term oscillations. However, the most puzzling feature of these climate proxies is the abrupt warming just after periods of slow cooling. Rapid warming is particularly well defined in the ice-core record: in some cases temperatures rise by several degrees within decades¹.

Orbital variations of insolation are obviously too slow and furthermore too limited in amplitude during the period¹² 60–20 kyr before present (BP) to account for such decade-to-century scale variability. Furthermore, massive iceberg discharge and climate variations seem to be linked in the palaeodata. Recently, model simulations have shown that massive iceberg discharges from the Laurentide ice sheet could not result directly from cooler temperatures over the Northern Hemisphere¹³. On the

FIG. 1 The ocean model is composed of three boxes: 1, high-latitude waters; 2, low-latitude surface; and 3, intermediate plus deep ocean. The fourth reservoir is the ice sheet of height H . The diffusive mixings k_{12} , k_{13} , k_{23} are constant, and the thermohaline circulation m is assumed to be proportional to the density difference between the two surface boxes, using a linear equation of state for sea water $m = \mu[\alpha(T_2 - T_1) - \beta(S_2 - S_1)]$, where T_i and S_i are the temperature and salinity of box i . In the atmosphere, the heat transport is $L = C_A(T_2 - T_1)$ and the water vapour is $V = C_V(T_2 - T_1)$. The snow accumulation is $A = C_A(T_2 - T_1)$, the melting is $M = C_M(T_1 - T_f)$ if $T_1 > T_f$. Where T_f is the melting temperature of ice (here 0°C), $M = 0$ otherwise. Iceberg calving is $I = 0$ when the ice sheet is growing and $I = -V/\tau$ during iceberg discharges. The net radiation fluxes are $Q_1 = Q_1^0 - q_1 T_1$ and $Q_2 = Q_2^0 - q_2 T_2$. The temperature profile in the ice sheet is parametrized by $T(z) = T(H) + \theta^2(1 - z/H)/(\theta + (\gamma - \theta)z/H)$, where $\theta = T(0) - T(H)$, $T(H) = T_1 + C_T - \Gamma H$, and γ is the temperature gradient at the base of the ice sheet imposed by the geothermal flux and, during surges, friction. (See Table 1 for definitions of symbols.)

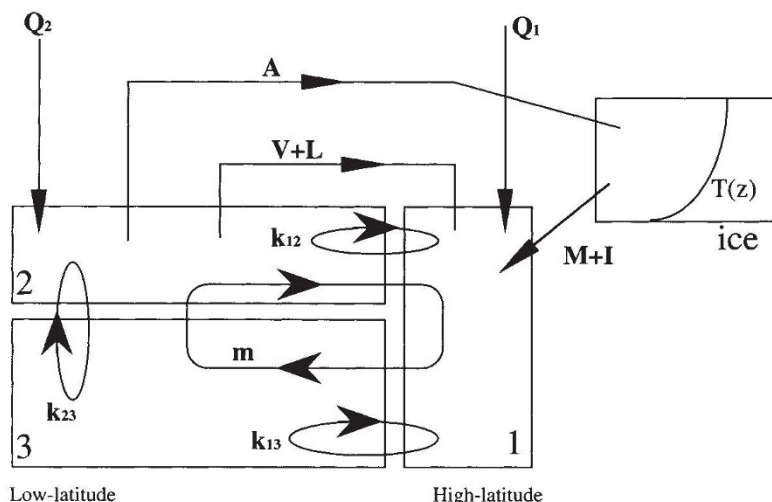


TABLE 1 Parameter values

Parameter	Value	Unit
V_1	20	10^6 km^3
V_2	20	10^6 km^3
V_3	200	10^6 km^3
k_{12}	6	Sv
k_{13}	10	Sv
k_{23}	10	Sv
μ	10,000	$\text{Sv m}^3 \text{ kg}^{-1}$
Q_1^0	-4.8	10^{15} W
Q_2^0	6	10^{15} W
q_1	-0.04	10^{15} W K^{-1}
q_2	-0.04	10^{15} W K^{-1}
F_G	0.05	W m^{-2}
Γ	9	K km^{-1}
C_T	6	K
τ	1,000	yr
C_A	0.0025	Sv K^{-1}
C_M	0.002	Sv K^{-1}
C_L	0.095	10^{15} W K^{-1}
C_V	0.037	Sv K^{-1}

Symbols used: V_1, V_2, V_3 are the volumes of the oceanic boxes; k_{12}, k_{13}, k_{23} the diffusive fluxes; μ the thermohaline circulation coefficient; Q_1^0, Q_2^0, q_1, q_2 the radiative coefficients; F_G the geothermal flux; Γ the atmospheric lapse rate; C_T the continental temperature effect; τ the surge time constant; C_A the accumulation coefficient; C_M the melting coefficient; C_L the meridional heat flux coefficient; C_V the meridional water vapour flux coefficient.

other hand, it has been shown that ice sheets (or at least ice-sheet models) can undergo internal oscillations^{14,15}, and it has been suggested that these oscillations could induce the climate changes associated with Heinrich events^{15,16}.

Such rapid climate warmings are nevertheless rather difficult to explain. The ocean probably plays a considerable part. Simple ocean box-models¹⁷ up to coupled ocean-atmosphere general circulation models¹⁸ show that thermohaline circulation in the North Atlantic region may exhibit two stable regime of flow. An 'off-mode' with a greatly reduced deep-water production in polar regions; and an 'on-mode' with an active deep-water formation and an efficient northward transport of heat and salt: high-latitude temperatures are then higher. A 'turn-on' or a 'turn-off' of the circulation is possible by changing the salinity budget at high latitudes, induced by evaporation, precipitation or runoff. The concept of a 'salt-oscillator' has already been proposed to explain the climate variations found in glacial time^{6,19}: abrupt cooling or warming is possible in only a few decades by changing slightly the freshwater budget.

Following these ideas, two tentative explanations have been proposed to explain the abrupt warming after Heinrich events, both involving an increase in the salinity of the North Atlantic, and thus a strengthening of the thermohaline circulation. Bond *et al.*⁵ suggest that, after the collapse of the ice sheet and the subsequent retreat of the ice margin, the flux of icebergs to the ocean is much reduced and the salinity is then allowed to increase. On the other hand, the fact that the high elevation of the Laurentide ice sheet is responsible for increased northerly winds over the western part of the North Atlantic, which considerably cools the surface waters during glacial time²⁰, led MacAyeal to suggest¹⁶ that its reduced elevation after collapse could induce a warming of surface waters, and consequently enhance the evaporation and the salinity.

Proxies for glacial palaeoceanography²¹ indicate that, during glacial periods, deep-water formation occurred mainly in the North Atlantic around 50° to 60° N. A large proportion of the icebergs associated with Heinrich events will melt in the same general area¹⁰ and will therefore have a considerable influence on the thermohaline engine. Here we explore the idea of Bond *et al.*⁵ using a numerical model coupling an oscillating ice sheet

with a bimodal ocean-atmosphere system. A schematic representation is shown in Fig. 1.

The ice-sheet is a zero-dimensional simplification of MacAyeal's model¹⁵, using a standard Galerkin method. The ice-sheet model oscillates between a growth phase and a surging phase, initiated by basal ice melting and subsequently stopped by basal ice freezing. During ice-sheet growth, we use the full advective-diffusive equation from MacAyeal's model, whereas during surges we consider only the downward advection of ice. The mass balance of the ice sheet is determined by the difference between accumulation and melting plus ablation. The ocean model is derived from Birchfield's three-box model¹⁷. It contains a low-latitude surface, a deep plus intermediate and a high-latitude box as shown in Fig. 1. Equations for temperature and salinity in each box are obtained by taking the balance of sources and sinks. Unlike Birchfield, we use an upstream advection scheme, though this is not crucial for the final result. Using the parameter values listed in Table 1, the model is integrated from an arbitrary initial condition for 50 kyr in order to eliminate transient behaviour, then for another 50 kyr to obtain the oscillations shown in Fig. 2. Vertical density stratification between boxes 2 and 3 always remains stable.

The role of the ocean is most easily seen in Fig. 3. Starting from a growing ice sheet and an active thermohaline circulation, ice-sheet melting brings only small quantities of fresh water to the high-latitude ocean. When the ice sheet collapses due to basal melting, a huge additional freshwater flux from iceberg calving and subsequent melting damps the circulation. This causes high-

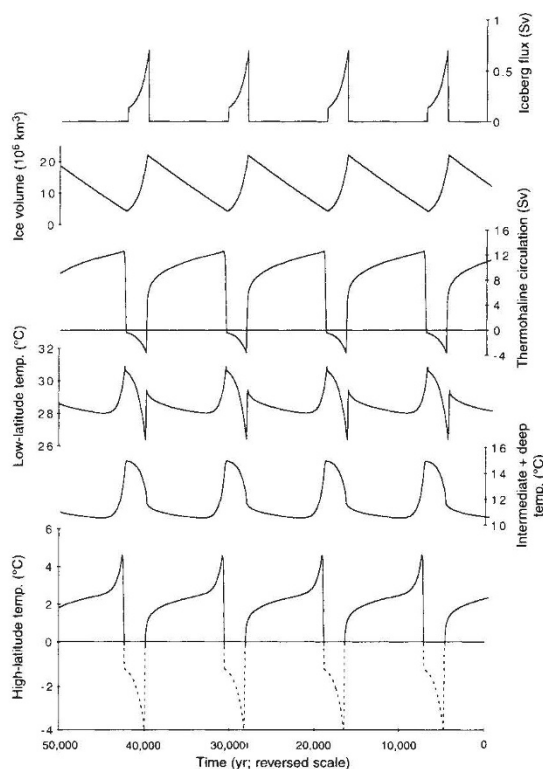


FIG. 2 Time evolution of the iceberg flux (in sverdrups, $10^6 \text{ m}^3 \text{ s}^{-1}$), the ice-sheet volume, the thermohaline circulation, and the temperatures of each box. Massive iceberg discharges stop the thermohaline circulation thus warming the low-latitude boxes while cooling the high-latitude box. The dashed line indicates sea-ice formation, which is equivalent to taking the high-latitude temperature curve as the heat content of the northern box. Just after the 'Heinrich event', the heat stored at low latitudes is brought to higher latitudes, resulting in an abrupt warming (over ~ 100 yr). Afterwards, the system slowly relaxes to what would be the equilibrium in the absence of the ice sheet.

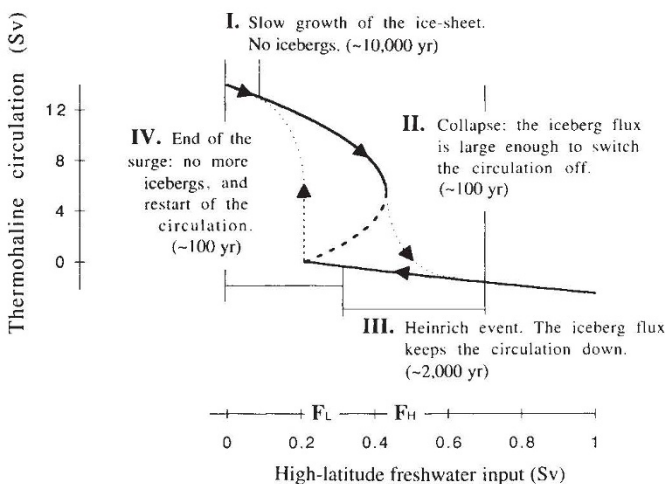


FIG. 3 The equilibrium value of the thermohaline circulation for the three-box ocean-atmosphere model alone (decoupled from the ice-sheet dynamics), plotted here as a function of the non-atmospheric freshwater flux (ice sheet and iceberg melting) to the high-latitude box. The successive phases of one oscillation are indicated. A transition from the 'on-mode' to the 'off-mode' occurs when the iceberg flux exceeds the high-threshold value F_H , and the opposite transition occurs when no more icebergs are produced, the freshwater flux being then below the low-threshold value F_L .

latitude cooling and low-latitude warming (Fig. 2) because of reduced meridional heat exchange: this temporary heat storage in low latitudes is essential for the subsequent warming at high latitudes. When the ice-sheet basal freezing interrupts the iceberg flux, the freshwater input comes back to its initial value and the thermohaline circulation restarts abruptly, bringing to higher latitudes the heat previously stored during the 'off' phase.

The abrupt climate changes present in our model correspond to the transient behaviour of a bimodal atmosphere-ocean system, influenced by periodic massive iceberg discharges. The direct melting of the ice sheet (M in Fig. 1) has here no essential role, in contrast to other models of glacial oscillations^{22,23}. Note also that no attempt whatsoever has been made to fit closely the palaeodata. In particular, the periodicity of the oscillations depends, as in MacAyeal¹⁵, on the parameter values chosen for the geothermal gradient, ice accumulation and ablation, and it varies between 5 and 30 kyr. The value of 11,750 yr found here has no particular significance. Likewise, an iceberg flux of a few tenths of a sverdrup ($1 \text{ Sv} = 10^6 \text{ m}^3 \text{ s}^{-1}$) is compatible with the surface-water $\delta^{18}\text{O}$ excursions of 1–2‰ found during 'Heinrich events'⁵, representing a 20 to 40 times dilution of ice with a $\delta^{18}\text{O}$ of -35‰: for a 100-m-deep surface layer covering $6 \times 10^6 \text{ km}^2$ of the North Atlantic and mixed over a 10-year period, an excess 2–5 m of fresh water corresponds indeed to a 0.5–1 Sv flux.

Thus, perhaps the simplest possible model coupling the ocean-atmosphere system with an ice sheet undergoes oscillations that have some common features with palaeoclimate records. In particular, we observe an abrupt warming in high-latitude regions just after the massive iceberg discharges from the ice sheet. Although this model is probably too simplistic to predict any numerical value, it nevertheless demonstrates the effect that the interactions between ice-sheet dynamics and the deep ocean circulation have on the variability of climate. □

Received 27 April; accepted 10 October 1994.

1. Johnsen, S. J. *et al. Nature* **359**, 311–312 (1992).
2. Dansgaard, W. *et al. Nature* **364**, 218–220 (1993).
3. Heinrich, H. *Quat. Res.* **29**, 142–152 (1988).
4. Bond, G. *et al. Nature* **360**, 245–249 (1992).
5. Bond, G. *et al. Nature* **365**, 143–147 (1993).

6. Broecker, W. S., Bond, G., Klas, M., Bonani, G. & Wolffli, W. *Paleoceanography* **5**, 469–477 (1990).
7. GRIP project members *Nature* **364**, 203–207 (1993).
8. Grootes, P. M., Stuiver, M., White, J. W. C., Johnsen, S. & Jouzel, J. *Nature* **366**, 552–554 (1993).
9. Jouzel, J. *et al. Nature* **329**, 402–408 (1987).
10. Grousset, F. E. *et al. Paleoceanography* **8**, 175–192 (1993).
11. Guiot, J. *et al. Palaeogeogr. Palaeoclimatol. Palaeoecol.* **103**, 73–93 (1993).
12. Berger, A. L. *J. Atmos. Sci.* **35**, 2362–2367 (1978).
13. Oerlemans, J. *Nature* **364**, 783–786 (1993).
14. Oerlemans, J. *Tellus* **35A**, 81–87 (1983).
15. MacAyeal, D. R. *Paleoceanography* **8**, 767–773 (1993).
16. MacAyeal, D. R. *Paleoceanography* **8**, 775–784 (1993).
17. Birchfield, E. *Clim. Dyn.* **4**, 57–71 (1989).
18. Manabe, S. & Stouffer, F. J. *Nature* **364**, 215–218 (1993).
19. Birchfield, E. G. & Broecker, W. S. *Paleoceanography* **5**, 835–843 (1990).
20. Manabe, S. & Broccoli, A. J. *Geophys. Res.* **90**, 2167–2190 (1985).
21. Labeyrie, L. D. *et al. Quat. Sci. Rev.* **11**, 401–413 (1992).
22. Wang, H., Birchfield, E. & Rich, J. in *Ice in the Climate System* (ed. Peltier, R.) 237–254 (NATO ASI Ser. I12, Springer, Berlin, 1993).
23. Birchfield, E., Wang, H. & Rich, J. *J. Geophys. Res.* **99**, 12459–12470 (1994).

ACKNOWLEDGEMENTS. We thank J. Jouzel, J. C. Duplessy, E. Birchfield and G. Bond for their comments on the manuscript.

Melt topology in partially molten mantle peridotite during ductile deformation

Zhen-Ming Jin*, Harry W. Green & Yi Zhou

Institute of Geophysics and Planetary Physics and Department of Earth Sciences, University of California, Riverside, California 92521, USA

THE process by which basaltic melt is generated and extracted beneath mid-ocean ridges is poorly understood. Knowledge of the distribution of melt within the parent mantle peridotite during the early stages of melting is important for interpretation of geophysical experiments and for construction of models of magma coalescence and extraction^{1–4}. Static experiments on mantle rocks and selected analogue materials have shown that, for small melt fractions, melt is concentrated along three-grain intersections, forming an interconnected web of tubes^{5–9}. Low-pressure deformation experiments on olivine + melt specimens have yielded the same conclusion^{10,11}. But in similar experiments on salt-brine mixtures during ductile deformation, the fluid emerges from the triple junctions where it resides under static conditions and spreads onto grain boundaries^{12–16}. Here we report the results of low-stress deformation experiments on partially molten peridotite at mantle temperatures and pressures, which show that such dynamic melting produces microstructures analogous to those of the salt-brine experiments. The very low viscosity of these specimens suggests that in the Earth, dynamic wetting could lead to melt separation at very low melt fractions, and to melt focusing at ridges.

Although many static partial-melting experiments have been performed on mantle compositions under mantle conditions^{5,9}, previous dynamic experiments have been conducted at ambient or low pressures on bulk chemistries significantly different from the primary peridotite of the Earth's mantle^{10,11,17}, or at stresses ~100 times those expected in the mantle¹⁸. At low pressures, the mineralogy of peridotite is different from that at the depths of melting in the Earth (the pyroxenes and aluminous phases change with pressure), and under high effective stresses melt-induced microcracking occurs. There is therefore a need for dynamic experiments more closely approaching the physical and chemical conditions in the mantle. Taking advantage of our molten-salt cell^{19,20} that allows low-stress deformation to be

* Permanent address: Division of Geomechanics, China University of Geosciences, Wuhan 430074, People's Republic of China.